Role of intermediate-range order in predicting the fragility of network-forming liquids near the rigidity transition

D. L. Sidebottom and S. E. Schnell

Phys. Rev. B **87**, 054202 — Published 15 February 2013

DOI: 10.1103/PhysRevB.87.054202

The Role of Intermediate Range Order in Predicting Fragility of Network-Forming Liquids near the Rigidity Transition

D. L. Sidebottom and S. E. Schnell
Department of Physics, Creighton University, Omaha, Nebraska 68178

Studies of network forming oxide liquids are combined with studies of network-forming chalcogenide glasses to demonstrate a universal dependence of the glass forming fragility on the topological connectivity of the network. This connection between structure and dynamics is congruent with theoretical predictions for a rigidity transition near an average bond number of 2.4 and the common pattern of fragility may be traced via a simple two-state bond model to a common variation of configurational entropy with connectivity. However, in order for this universality to appear the connectivity of the oxide networks must be defined in a progressive manner that accommodates the presence of those rigid structural units which comprise both the short range and intermediate range order. Replacement of these robust structural units by equivalent network nodes is necessary but can be viewed as a coarse-graining of the network to a bond lattice of weakest links that are most relevant to zero-frequency properties like the fragility.

PACS# 61.20.-p, 61.43.Fs, 64.60.aq, 64.70.ph

I. Introduction

Even the Ancients understood that the properties of a glass depend upon its chemical composition and quality of ingredients[1]. The addition of sodium oxide to silica, for example, reduces the number of bridging oxygen bonds in the network structure. This weakens the network and results in a lowering of the glass transition temperature, T_g. Conversely, calcium oxide can then be added to this damaged network to improve chemical durability and reduce water solubility. Moreover, other oxide glass formers like B_2O_3, can be combined with silica to produce glasses with improved tolerance to thermal stress. Indeed, these chemical modifications alone result in the well known soda-lime silicates and borosilicates that are the foundation for almost all commercial glass products being manufactured today[1,2].

But these same chemical modifications also affect the viscous properties of the glass forming melt just above T_g. For example, the addition of sodium oxide not only lowers the T_g, but also enhances the temperature range over which the viscosity remains low enough for the melt to be formed into a desired shape[1]. This "workability" of the melt is a complex function of the temperature and composition dependence of the viscosity but is also sensitive to the heat capacity and thermal conductivity. Clearly the industrial processing of glass products requires very accurate knowledge of both the thermal and viscous behavior of a melt with regards to both temperature and chemical composition and it is not surprising that the goal of many researchers[3] has been to develop a clearer theoretical understanding of the glass transition as well as a better understanding of

how glass forming dynamics may be related to the underlying chemical structure of the glass.

In this paper, we examine the connections between the *fragility* of network forming liquids and the degree of connectivity of their network structure. Fragility, to be defined momentarily, is a signature metric of glass forming dynamics and is seen to respond sharply to increased connectivity in both oxide glasses and chalcogenide glasses. Indeed, we demonstrate that the fragility decreases in an *identical* fashion with increasing connectivity of the network provided the network is coarse grained such that inflexible structural units that comprise either the short range or intermediate range order are treated as equivalent network nodes. The resulting "bond lattice" then reflects only those weakest connections of the network that participate in the low frequency deformations leading to viscous flow of the melt. We argue that this common dependence of fragility on network connectivity might be interpreted within the framework of a classical two-state model[4-6] in which a free energy, $\Delta G = \Delta H - T\Delta S$, separates the intact bond state from a thermally excited, broken bond state. In this model, the fragility is then determined solely by the entropy increase, ΔS, that represents the wealth of new configurations which become accessible when the bond is broken.

II. A. Dynamics and Fragility

The glass transition temperature is a conventional benchmark loosely defined as that temperature where the viscosity reaches 10^{15} Pa·s or the structural relaxation time, τ, is of the order of 100 seconds. With heating above T_g, both these

quantities decrease as the melt "unthickens" and it is the rapidity of this unthickening that is characterized by the fragility[7-9]. Although there are other ways of characterizing the fragility, the most widely adopted definition is that derived from a logarithmic plot of the relaxation time (or viscosity) against inverse temperature scaled to T_g. In this representation, the fragility is defined as the slope,

$$m = \left. \frac{\Delta \log \tau}{\Delta (T_g / T)} \right|_{T \to T_g}, \qquad (1)$$

near the glass transition temperature.

Glass forming melts with a high fragility (m > 80) are melts that unthicken rather abruptly when heated above T_g. This rapid unthickening is most common for a large number of simple molecular liquids (e.g., glycerol) that interact through reasonably weak bonding forces. By comparison, glasses that form a 3D network of covalent bonds have fragilities in a range from m = 20 to 30 and are often referred to as "strong" glass formers.

II. B. Structure and Rigidity Theory

Theoretical ponderings on the role of network connectivity in relation to elastic properties of a glass came of age with the advance of *rigidity theory* based upon constraint counting. Introduced by Phillips[10] and refined in later work by Thorpe[11,12], rigidity theory considers the topology of a 3D network consisting of N atoms of which a fraction, f_r, form r = 2, 3, 4, ... bonds to neighboring atoms. These bonds produce constraints in the system, and according to the theory, an atom with

$r \geq 2$ bonds has $r/2$ bond length constraints and $(2r\text{-}3)$ bond angle constraints[11]. The average number of constraints per atom is then given by

$$\sum_r f_r \{(r/2)+(2r-3)\} = \frac{5}{2}\langle r \rangle - 3, \qquad (2)$$

where $\langle r \rangle = \sum_r f_r r$ is the average bond number per atom. Of obvious interest is how the total number of constraints compares with the available degrees of freedom (equal to 3 per atom). If the constraints outweigh the degrees of freedom, then the network is over constrained or *rigid*. Conversely, if the constraints are fewer than the degrees of freedom, then the network is under constrained or *floppy*. One can easily show that the transition between rigid and floppy then occurs when $\langle r \rangle$ = 2.4.

Early simulations by He and Thorpe[12] largely confirmed the existence of a transition but it was only later that the theory was applied to real amorphous materials that form covalently-bonded networks. In work by Halfpap[13] and later by Tatsumisago[14] and Boehmer[15], researchers investigated the glass forming properties of a series of so-called *chalcogenide* (group VI) glasses based on Se but doped with As and Ge. When Se (with r = 2) is doped with either As (r = 3) or Ge (r = 4), the average bond number can be varied continuously between $\langle r \rangle$ = 2 to about 2.7 while remaining within the glass forming range of this system. In this way, both the dynamics and thermodynamics of the glass could be monitored as the network evolved from one that is under constrained (floppy) to one that is over constrained (rigid).

Later extensions to the original theory include: (1) corrections for systems with $r = 1$ (so-called dangling bonds) that result in a shift of the transition point [16] and (2) emerging evidence that in many systems the transition between under constrained and over constrained is often separated by a so-called *intermediate phase* that is characterized by a vanishing non-reversing heat flow[17]. In even more recent work, the theory has been applied to the folding of proteins[18]

A particular consideration in the works by Tatsumisago[14] and Boehmer[15] was the dependence of the fragility of these chalcogenide liquids as a function of network structure. Their results are reproduced in Fig. 1 and show that the fragility of these network forming glasses is reasonably high, with $m \approx 80$ for amorphous Se (polymeric with $\langle r \rangle = 2$), but decreases rapidly between $\langle r \rangle = 2$ and $\langle r \rangle = 2.2$ then less rapidly thereafter as additional covalent bonds are introduced. A slight minimum was reported[15] at the critical $\langle r \rangle = 2.4$, but for $2.3 < \langle r \rangle < 2.7$ the fragility remains reasonably constant around $m = 33 \pm 3$. Although rigidity theory makes no specific prediction for the fragility, this trend in which $\langle r \rangle \approx 2.4$ separates the weaker, under constrained networks that are fragile from the over constrained networks that are non-fragile resonates well with the principles of the theory.

II. C. Bond Lattice Model

To address the fragility in these network forming glasses, one needs to model the developing fluidity that arises when some fraction of bonds are being broken as a result of increased thermal energy. The simplest model is a classic two-state

model[4-6] in which each connecting bond can be either intact or broken. These two states are separated by a free energy barrier, $\Delta G = \Delta H - T\Delta S$, and at thermal equilibrium, the fraction of broken bonds is given by[4]

$$X_B = \left(1 + \exp\left(\Delta G / RT\right)\right)^{-1}. \quad (3)$$

Here, the enthalpy change ΔH is largely determined the by the strength of the covalent bond while ΔS is a measure of the entropy gain, in the form of increased conformations that become available, when the constraint is removed.

In the model, the probability for a rearrangement of atoms to occur such that viscous flow may proceed is given by [5]

$$P(T) \propto \tau^{-1} \approx \Omega \exp\left(-f^* / X_B\right), \quad (4)$$

where *f** represents some critical fraction of broken constraints (often taken as unity). Angell and coworkers[5,6] have studied the bond lattice model numerically and have concluded that the liquid's fragility is determined entirely by the magnitude of ΔS. This then offers some insight into the dependence of the fragility of the chalcogenides on the average bond number. Near and above $\langle r \rangle$ = 2.4, where the network is either critically constrained or over constrained, the presence of redundant constraints means that the removal of a single bond produces very little in the way of additional configurations the system can access. Here, ΔS is very small and so too is the fragility. But as the system becomes under constrained, removal of a single bond can release a sizable number of accessible configurations. ΔS then increases with decreasing bond density and, within the framework of the bond lattice model, is mirrored by the increasing fragility seen experimentally.

III. A. Phosphate Networks

We believe this connection between fragility and configurational entropy helps us to understand the results of a recent dynamic light scattering (DLS) study of sodium phosphate glass forming melts[19]. Unlike the chalcogenide system discussed above, these phosphate melts form an oxide network filled with *P-O-P* bonds whose number can be manipulated through the addition of an alkali oxide. Here, it is customary for glass scientists to describe the structure of an oxide network as composed of discrete *structural units* (building blocks of well-defined short range order (SRO)) that are interconnected through bridging oxygen bonds. The basic structural building block of the oxide network in alkali phosphate glasses, such as $(Na_2O)_x(P_2O_5)_{1-x}$, is the PO_4 tetrahedron[20] illustrated in the inset to Fig. 1. In pure P_2O_5 ($x = 0$), each PO_4 unit forms three bridging oxygen bonds to neighboring phosphor atoms (NMR spectroscopists often refer to this as a Q^3 configuration) while the forth oxygen is double bonded and non-bridging. Addition of Na_2O brings about the cleavage of a single bridging oxygen bond with a uniform conversion of the PO_4 units from Q^3 to Q^2, each having only 2 bridging oxygen bonds. Thus the network of bridging oxygens is transformed from a 3D continuous random network (CRN) (present at $x = 0$) to a system of linear $[PO_4]_n$ polymer chains at the metaphosphate ($x = 0.5$) composition. The compositional fractions of Q^3 and Q^2 units in the phosphate system are well established[20] as,

$$f_2 = \left(\frac{x}{1-x}\right) \quad \text{and} \quad f_3 = \left(\frac{1-2x}{1-x}\right), \tag{5}$$

and the average bridging oxygen bond number is given simply as $\langle n \rangle = 2f_2 + 3f_3$.

Considering how this phosphate network would respond to those low frequency deformations that contribute to viscous flow, we might anticipate that the *PO4* units remain largely inflexible in the sense that their *P-O* bond length and angles would be unaffected. That is, the *PO4* would behave as a rigid structural unit that maintains its tetrahedral shape. Instead, the flexure would occur mainly at the oxygen bridge between *PO4* units and viscous flow would be controlled almost entirely by the thermal disruption of these same bridging bonds. We would then expect the bond lattice relevant for the two-state model to be obtained by coarse graining out the *PO4* structural units and replacing them with an equivalent network node. In this way, the structures of both the sodium metaphosphate with $\langle n \rangle = 2$ and amorphous selenium with $\langle r \rangle = 2$ would appear topologically equivalent (i.e., each is composed of polymer chains) and may be expected to share similar properties in terms of their configurational entropy.

In fact, this seems to be born out in Fig. 1 where the fragility of the sodium phosphate liquids exhibit *exactly* the same dependence on lattice connectivity (measured by $\langle r \rangle$ or $\langle n \rangle$, respectively) including even a minor minimum in the vicinity of $\langle n \rangle = 2.4$. Again, within the framework of the bond lattice model[6], the fragility is directly dependent on the amount by which configurational entropy is changed when a single connection is removed. Here we conclude that this ΔS is the same for these two topologically equivalent networks and so too is the fragility.

Additional support is provided by an even more recent light scattering investigation[21] of aluminophosphate melts which are included in the figure. In

this instance, there occurs a conversion from Q^2 to Q^6 as PO_4 units are replaced by six-coordinated AlO_6 units when aluminum metaphosphate is substituted for sodium metaphosphate[22,23]. The average bridging oxygen bond density can be obtained as $\langle n \rangle = 2f_{PO4} + 6f_{AlO6}$, where the fractions of PO_4 and AlO_6 have been determined by NMR[23] studies and again, when the network is coarse grained in such a manner to replace the rigid, structural units comprising the SRO by equivalent network nodes, a common dependence of the fragility on lattice connectivity emerges.

Before proceeding, we pause briefly to address a handful of potential issues that might be raised. Firstly, in our analysis we have tacitly assumed that the fragility we obtain from the structural relaxation probed by DLS is equivalent with that obtained from the viscosity. In principle, the VV light scattering we analyze is influenced by any orientational motion that may be present in addition to the structural relaxation[24] and so the proportionality between our relaxation time and the viscosity is not ensured. However, it is unlikely for these covalent networks to exhibit any significant decoupling of rotational motion from structural relaxation and, since there are many experimental examples in the literature[25,26] for which the relaxation time is observed to parallel the viscosity, we believe our assumption is justified.

Secondly, we should emphasize that our picture of the coarse graining is one in which the network of robust structural units (e.g., PO_4) are linked together by weaker bridging oxygen bonds to form the bond lattice whose connectivity is characterized by the density of these linkages, $\langle n \rangle$. Just above T_g, it is these weak

linkages between structural units that first break to give rise to viscous flow while those bonds internal to the structural units remain largely intact. Obviously, at some very high temperature these structural units will eventually lose their integrity with internal bonds being broken. But this would only happen at temperatures far from T_g and thus far from the region in which the fragility is defined.

Lastly, the approach we have taken should not be viewed as merely an extension of the sort of modifications to rigidity theory developed by Boolchand and coworkers[27] mentioned previously. There, rigidity theory has been augmented to accommodate dangling bonds (with r =1) as well as contributions to $\langle r \rangle$ from those loose alkali ions that are responsible for the formation of non-bridging oxygens[28] and these modifications have helped in understanding certain thermal and vibrational properties that constitute the so-called intermediate phase. However, the underlying approach to counting constraints in these studies remains one that is based upon an atomic-level enumeration of the average bond density - an approach that does not separate off those bonds that comprise the short range order as does our current coarse-graining approach. It seems that while certain thermal and vibrational properties may be better described by the connectivity at all scales (both local and long range), the low frequency deformations of the network that contribute to the fragility are better understood using a bond lattice in which rigid structural units are treated as equivalent network nodes.

III. B. Borate Networks

In an effort to evaluate the generality of our finding shown in Fig. 1, we turn now to yet another network forming oxide system, namely the alkali-modified borate glasses of the form $(M_2O)_x(B_2O_3)_{1-x}$. B_2O_3 forms a network of BO_3 units with Q^3 bridging connectivity[29]. But unlike the phosphate liquids which suffer a reduction in bridging oxygen bonds and a decrease of $\langle n \rangle$ with the addition of alkali, the initial addition of alkali to B_2O_3 results in the replacement of three-coordinated boron (BO_3 units) by four-coordinated boron (BO_4 units described as Q^4)[29] that *reinforce* the network by increasing the value of $\langle n \rangle$.

Naturally, it was our expectation that the fragility of alkali borate melts would decrease with increasing $\langle n \rangle$. However, measurements of the fragility obtained from the viscosity of both lithium borate[30] and sodium borate[31,32] melts clearly indicate the fragility *increases* with alkali addition up to concentrations of x = 35 mol% alkali oxide. In fact, when the fragility are plotted as a function of $\langle n \rangle = 4\left(\frac{x}{1-x}\right)+3\left(\frac{1-2x}{1-x}\right)$ as is done in Fig. 2, it is clearly evident that they share no similarity with the pattern seen earlier for the chalcogenides and the phosphates. Equally peculiar is the odd "dogleg" seen for m vs. $\langle n \rangle$ (i.e, in advance of $\langle n \rangle$ = 3.3 the fragility increases rapidly but then abruptly plateaus at $m \approx 60$ between 3.3 to 3.5) that occurs in this region far removed from the rigidity transition point.

A puzzle immediately presents itself. How can the fragility of the borate network increase as more bonds are being introduced - a trend that is precisely opposite what we observed for the phosphate and chalcogenide networks? Some have recently shown[32,33] that the increasing fragility in the borates may be

modeled by introducing into rigidity theory constraints that are thermally switched on or off. In this approach, constraints are enumerated on an atom-by-atom basis (i.e., using $\langle r \rangle$ as was done above for the chalcogenides) but each constraint is also assigned a special temperature above which the constraint becomes broken. For the borate system, the model can account for the compositional variation of the glass transition temperature nicely, but despite the added flexibility afforded by the thermally activated constraints, it provides only a qualitative description of the fragility[32].

Motivated by our success in using $\langle n \rangle$ as a means of coarse-graining the phosphate network to achieve what seemed to be the proper characterization of network connectivity (at least that relevant for zero frequency modes of deformation), we have chosen to explore an alternative resolution to this puzzle and seek to identify some special feature unique to the borate network that might account for the discrepancy. One prominent feature that distinguishes the borate glass structure from other oxide network-forming glasses is its tendency to form well-documented[28,34,35] intermediate range order (IRO). Both Raman spectroscopy[36,37] and NMR[35,38,39] studies have repeatedly concluded that some fraction of the BO_3 units in B_2O_3 reside in 6-membered "boroxol" rings (see inset of Fig. 3). The presence of these rings is signaled by a very sharp Raman line centered near 808 cm^{-1}[36] caused by a symmetric breathing mode that suggests the rings form a robust, rigid substructure of the network. Although the actual proportion of boron atoms participating in rings has been a matter of some debate

in the past, more recent evidence[40,41], including a first-principles molecular dynamics simulation[42], support a fraction somewhere between 60 to 75%.

In addition to the boroxol rings found abundantly in B_2O_3, other robust superstructures (mainly the diborate and tetraborate units shown in the inset of Fig. 3) are known to develop with the addition of alkali ions. The earliest models of this IRO structure were developed by Krogh-Moe[34] nearly 50 years ago and modern NMR measurements such as those on potassium borates by Youngman and Zwanziger[35] shown in Fig. 3, reaffirm that the borate structure (at least for $x < 33$ mol%) can be well accounted for using a collection of just five structural units: loose BO_3, loose BO_4, boroxol rings, tetraborate units and diborate units. The fraction of all boron atoms participating in each of these structures (f_3, f_4, f_B, f_T, and f_D, respectively) was determined from the NMR study and is presented here in Fig. 3 as a function of the mole percent of K_2O.

We believe it is the unique IRO of the borate network that causes its fragility to increase despite the increasing connectivity of the boron atoms. How does this happen? We will argue again, that in the same manner in which the SRO of the phosphate glasses was sufficiently robust as to be impervious to the long wavelength deformations that result in viscoelastic flow of the liquid and which in turn determine the liquid's fragility, so too are the superstructural units that make up the IRO of the borate network. Thus, if a means can be found to coarse-grain the network at yet another level so that the superstructual units associated with the IRO are likewise replaced by equivalent network nodes, then it may be possible to

achieve a lowering of the bond lattice connectivity (despite the increased coordination of the boron atoms) that would resolve the puzzle.

As way of an illustration, consider first the boroxyl rings that comprise roughly 65% of the boron atoms in B_2O_3. Replacing each ring with an equivalent node would result in an object that has three bridging bonds to the surrounding network. As each ring has 3 boron atoms, it would *seem* appropriate to assign an effective bond number $n_{eff} = 1$ to those boron residing in rings while assigning $n_3 = 3$ to remaining 35% of the boron that exist in loose BO_3. This would then result in $\langle n \rangle_{IRO} = 3(0.35) + 1(0.65) = 1.7$ for B_2O_3. While this has produced the lowering of the connectivity we desire, it incorrectly implies that the 65% of the boron atoms form *dangling* bonds that serve no function in connecting one part of the network to another. Instead we propose to view each boron atom in the ring as a two-sided link with $n_{eff} = n_B = 2$ because each serves to connect the outside network to the ring/node itself. Adopting this recipe, we would characterize the connectivity of the B_2O_3 network by $\langle n \rangle_{IRO} = 3(0.35) + 2(0.65) = 2.35$ which places the fragility ($m \approx 33$) in reasonable agreement with those data in Fig. 1.

By similar reasoning, each boron in a diborate unit (see inset to Fig. 4) would then be assigned $n_D = 2$, while those in the tetraborate structure are assigned $n_T = 1.5$. In the case of the tetraborate, only six of the eight boron atoms in this structural unit function as links to the external network and each of these is again assigned $n_{eff} = 2$. However, since the other two boron atoms that reside entirely within the tetraborate unit provide no added connectivity between the tetraborate unit itself

and the external network, they would be assigned $n_{eff} = 0$. Hence we arrive at an effective bond number for those boron atoms in a tetraborate of $n_T = (6 \times 2)/8 = 1.5$.

Together with loose BO_3 ($n_3 = 3$) and loose BO_4 ($n_4 = 4$), we can now test the prediction for a coarse grained connectivity given by $\langle n \rangle_{IRO} = 2f_B + 1.5f_T + 2f_D + 3f_3 + 4f_4$, where the fractions of boron in each structural unit are taken directly from the NMR investigation[35] provided in Fig. 3. As shown in Fig. 4, our simple recipe indeed produces *exactly* the desired effect! The aforementioned dogleg has vanished leaving a monotonic dependence of m on $\langle n \rangle_{IRO}$ that coincides precisely with that of both the chalcogenide and phosphate glasses. We emphasize that this collapse of four different network-forming glasses is achieved using *no adjustable parameters*.

IV. Conclusions

What is the significance of this result? We believe the universal pattern seen for the chalcogenides, phosphates and borates in Fig. 4 arises from how each network has been properly *transformed* to an equivalent bond lattice consisting only of those weakest linkages whose rupture will contribute most to viscous flow. For any given value of the connectivity ($\langle r \rangle$, $\langle n \rangle$ or $\langle n \rangle_{IRO}$, depending on the rigid substructures present), these bond lattices share a common topology and therefore a similar sensitivity of the configurational entropy to the addition or removal of bonds. Within the framework of a simple two-state bond model, it is this configurational entropy that determines the fragility and thus accounts for the

pattern observed in Fig. 4. In this way we have uncovered a tangible relationship between the dynamics of a glass forming liquid and the underlying network structure of its solid counterpart based upon simple thermodynamic principles.

In summary, we find evidence for a universal relationship between the dynamics of a network forming liquid and the structure of the network itself. This relationship appears in the form of a common dependence of the fragility for chalcogenide, phosphate and borate glasses as a function of the average bond number for the corresponding bond lattice of weakest links. This bond lattice is derived from the original covalent network by coarse graining those rigid structural units that make up either the short range or intermediate range order into equivalent nodes in the lattice. Connections of this sort between dynamics and structure are rare, but are of fundamental importance for manufacturing concerns and for our general understanding of the glass transition.

Acknowledgement: We gratefully acknowledge the financial support of NSF (grant # DMR-0906640).

References

[1] J. Zarzycki, *Glasses and the vitreous state*, (Cambridge University Press, Cambridge 1991).

[2] S. R. Elliott, *Physics of amorphous materials, 2nd Ed*. (Longman Scientific and Technical, Essex 1990).

[3] P. W. Anderson, Science **267**, 1625 (1995).

[4] C. A. Angell, J. Phys. Chem. **78**, 3698 (1971).

[5] C. A. Angell and K. J. Rao, J. Chem. Phys. **57**, 470 (1972).

[6] C. A. Angell, B. E. Richards and V. Velikov, J. Phys.: Cond. Matt. **11**, A75 (1999).

[7] W. Oldekop, Glastech Ber. **8**, 30 (1957).

[8] W. T. Laughlin and D. R. Uhlmann, J. Phys. Chem. **76**, 2317 (1972).

[9] C. A. Angell, in *Relaxations in Complex Systems*, Proceedings of the Workshop on Relaxation Processes, Blacksburg, Virginia, 1983, Ed. by K. Ngai and G. B. Wright (National Technical Information Service, U.S. Dept. of Commerce, Washington, DC, 1985), p. 3.

[10] J. C. Phillips, J. Non-Cryst. Solids **34**, 153 (1979).

[11] M. F. Thorpe, J. Non-Cryst. Solids **57**, 355 (1983).

[12] H. He and M. F. Thorpe, Phys. Rev. Lett. **54**, 2107 (1985).

[13] B. L. Halfpap and S. M. Lindsay, Phys. Rev. Lett. **57**, 847 (1986).

[14] M. Tatsumisago, B. L. Halfpap, J. L. Green, S. M. Lindsay, and C. A. Angell, Phys. Rev. Lett. **64**, 1549 (1990).

[15] R. Boehmer and C. A. Angell, Phys. Rev. B **45**, 10091 (1992).

[16] P. Boolchand and M. F. Thorpe, Phys. Rev. B **50**, 10366 (1994).

[17] P. Boolchand, D. G. Georgiev and B. Goodman, J. Optoelectronics and Adv. Mat. **3**, 703 (2001).

[18] A. J. Rader, B. M. Hespenheide, L. A. Kuhn, and M. F. Thorpe, Proc. Natl. Acad. Sci. U.S.A. **99**, 3540 (2002).

[19] R. Fabian, Jr. and D. L. Sidebottom, Phys. Rev. B **80**, 064201 (2009).

[20] R. K. Brow, J. Non-Cryst. Solids **263&264**, 1 (2000).

[21] T. Tran and D. L. Sidebottom, manuscript in preparation.

[22] R. K. Brow, J. Am. Ceram. Soc. **76**, 913 (1993).

[23] R. K. Brow, R. J. Kirkpatrick and G. L Turner, J. Am. Ceram. Soc. **76**, 919 (1993).

[24] G. Fytas, C. H. Wang, D. Lilge, and T. Dorfmuller, J. Chem. Phys. 75, 4247 (1981).

[25] M. D. Ediger, C. A. Angell and S. R. Nagel, J. Phys. Chem. **100**, 13200 (1996).

[26] D.L. Sidebottom, R. Bergman, L. Börjesson, and L. M. Torell, Phys. Rev. Lett. **71**, 2260 (1993).

[27] M. Zhang and P. Boolchand, Science **266**, 1355 (1994).

[28] J. W. Zwanziger, S. L. Tagg, and J. C. Huffman, Scienced **268**, 1510 (1995).

[29] D. L. Griscom in *Borate Glasses: Structure, properties and applications* (Materials Science Research, vol 12). Edited by L. D. Pye, V. D. Frechette, and N. J. Kreidel. Plenum, New York, 1978.

[30] G. D. Chryssikos, J. A. Duffy, J. M. Hutchinson, M. D. Ingram, I. I. Kamitsos and A. J. Pappin, J. Non-Cryst. Solids **172-174**, 378 (1994).

[31] S. V. Nemilov, Neorg. Mater. **2**, 349 (1966).

[32] J. C. Mauro, P. K. Gupta, and R. J. Loucks, J. Chem. Phys. **130**, 234503 (2009).

[33] P. K. Gupta and J. C. Mauro, J. Chem. Phys. **130**, 094503 (2009).

[34] J. Krogh-Moe, Phys. Chem. Glasses **3**, 101 (1962); ibid. **6**, 46 (1965).

[35] R. E. Youngman and J. W. Zwanziger, J. Phys. Chem. **100**, 16720 (1996).

[36] G. E. Walrafen, S. R. Samanta, and P. N. Krishnan, J. Chem. Phys. **72**, 113 (1980).

[37] W. Konijnendijk and J. Stevels, J. Non-Cryst. Solids **18**, 307 (1975).

[38] G. Jellison, Jr. and P. Bray, J. Non-Cryst. Solids **29**, 187 (1978).

[39] P. Bray, S. Feller, G. Jellison, Jr., and Y. Yun, J. Non-Cryst. Solids **38-39**, 93 (1980).

[40] R.N. Sinclair, C.E. Stone, A.C. Wright, I.G. Polyakova, N.M. Vedishcheva, B.A. Sahkmatkin, S. Feller, B.C. Johanson, P. Venhuizen, and R.B. Williams, Phys. Chem. Glasses **41**(5), 286-289 (2000).

[41] I. Hung, A. P. Howes, B. G. Parkinson, T. Anupold, A. Samoson, S. P. Brown, P. F. Harrison, D. Holland, and R. J. Dupree, Solid State Chem., **182**, 2402–2408 (2009).

[42] G. Ferlat, T. Charpentier, A. P. Seitsonen, A. Takada, M. Lazzeri, L. Cormier, G. Calsas, and F. Mauri, Phys. Rev. Lett. **101**, 065504 (2008).

Figure Captions:

Fig. 1

The fragility of chalcogenide [15] (solid squares), sodium phosphate [19] (solid circles), and sodium aluminophosphate [21] (open circles) glass forming melts plotted as a function of the average bond number, $\langle r \rangle$ or $\langle n \rangle$ as defined in the text. The dashed line is a guide to the eye. Inset illustrates the network structures of the chalcogenides and of the phosphate oxide network containing PO_4 units with Q^3 and Q^2 as well as AlO_6 with $n = 6$

Fig. 2

The fragility of Li and Na-borate glasses[30,31] are seen to increase with $\langle n \rangle$ and fail to collapse onto the same curve of Fig. 1. Inset illustrates the network structures of the borate system containing BO_3 and BO_4 units.

Fig. 3

The fraction of boron atoms found in the various IRO superstructures of the borate glass system at selected concentrations of alkali oxide as reported by a recent NMR investigation[35]. These superstructures are illustrated in the inset. In addition to the loose BO_3 and BO_4 units, superstructural units include the boroxol ring (containing 3 boron), the tetraborate unit (containing 8 boron), and the diborate unit (containing 4 boron).

Fig. 4

The fragility of Li and Na-borate glasses[30,31] are shown to collapse onto the same curve of Fig. 1 provided the average bond number is defined to include the IRO of the network as discussed in the text. Inset illustrates how the superstructural units in the borate network are coarse-grained into equivalent network nodes.

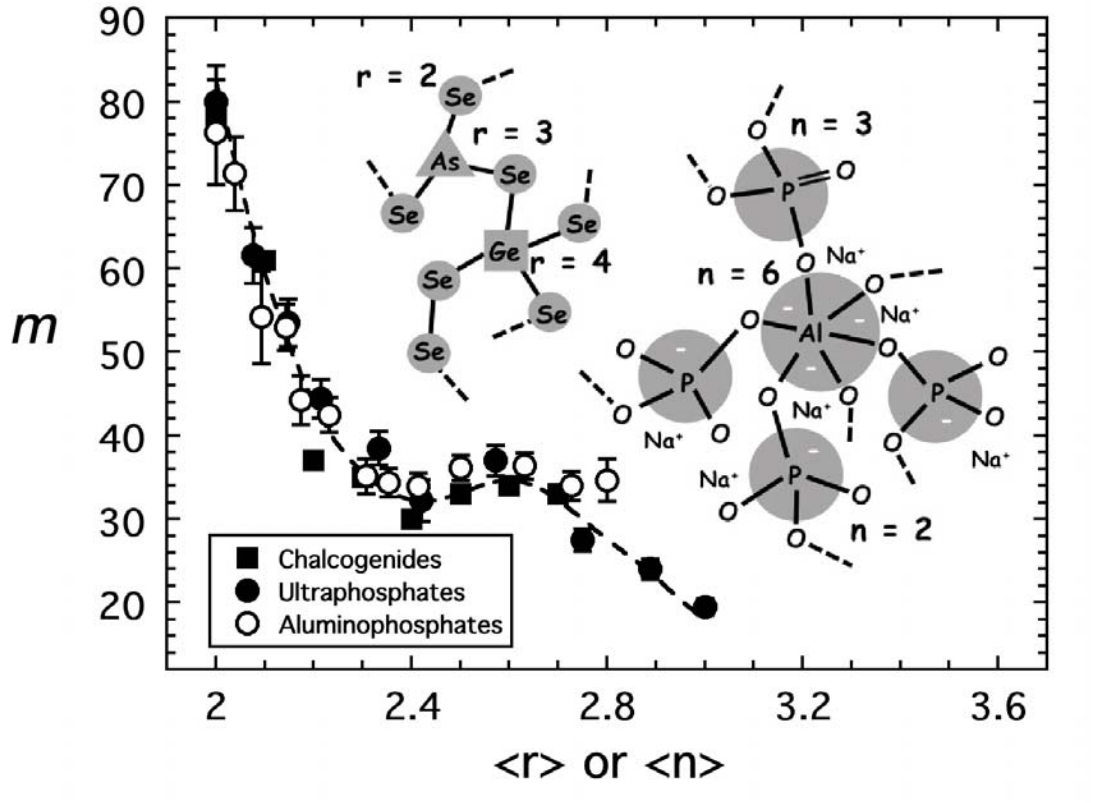

Figure 1

The fragility of chalcogenide [15] (solid squares), sodium phosphate [19] (solid circles), and sodium aluminophosphate [21] (open circles) glass forming melts plotted as a function of the average bond number, $\langle r \rangle$ or $\langle n \rangle$ as defined in the text. The dashed line is a guide to the eye. Inset illustrates the network structures of the chalcogenides and of the phosphate oxide network containing PO_4 units with Q^3 and Q^2 as well as AlO_6 with n = 6

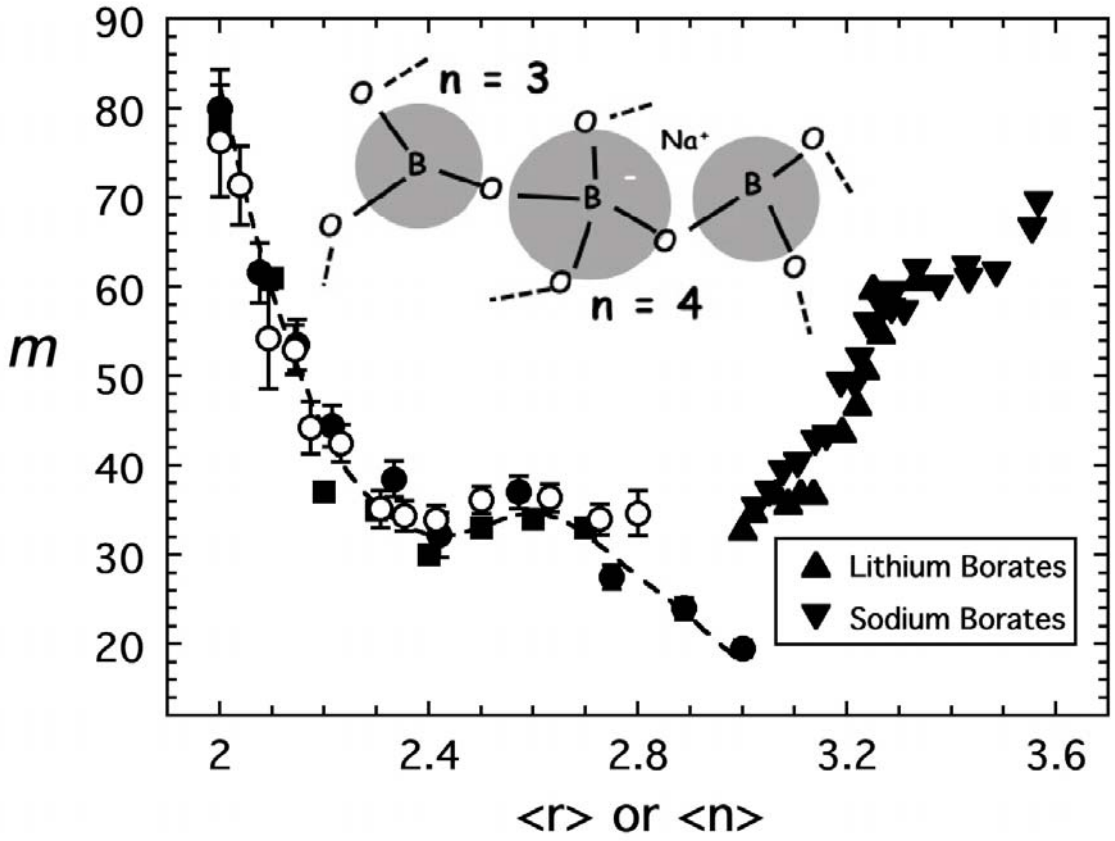

Figure 2

The fragility of Li and Na-borate glasses[30,31] are seen to increase with $\langle n \rangle$ and fail to collapse onto the same curve of Fig. 1. Inset illustrates the network structures of the borate system containing BO_3 and BO_4 units.

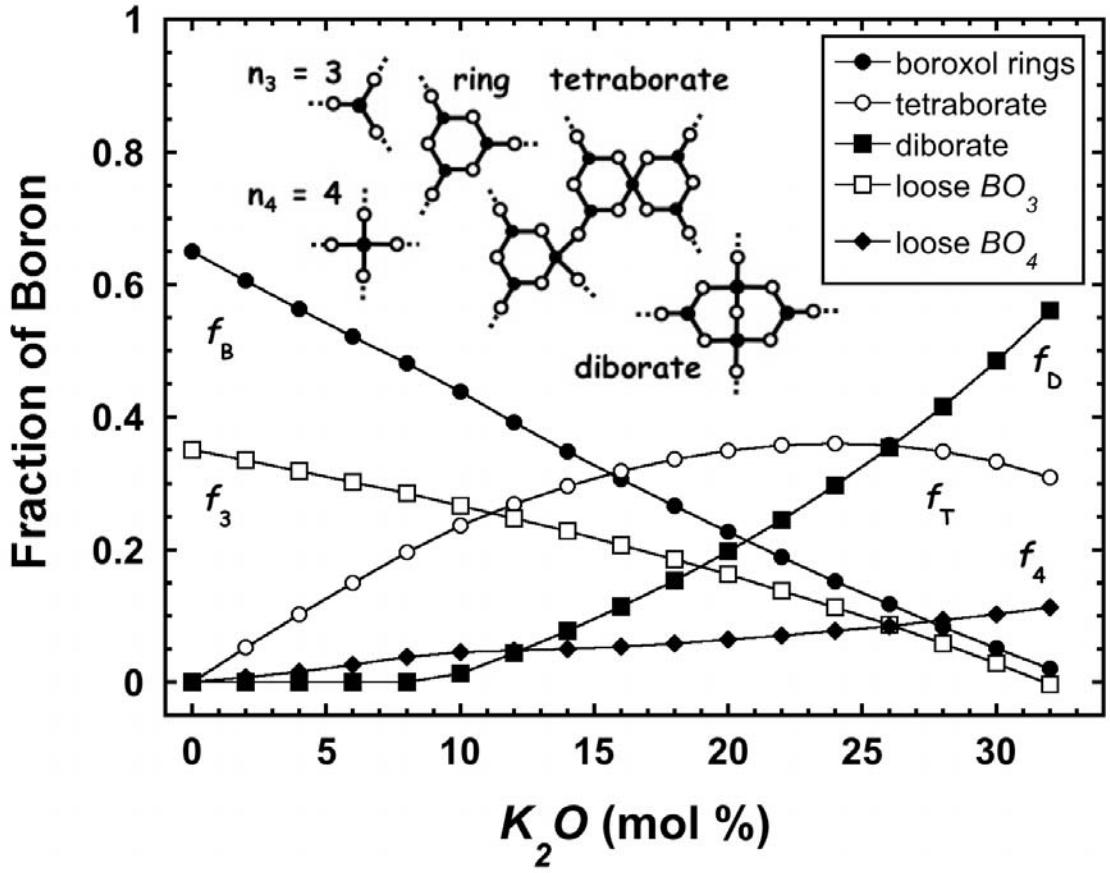

Figure 3

The fraction of boron atoms found in the various IRO superstructures of the borate glass system at selected concentrations of alkali oxide as reported by a recent NMR investigation[35]. These superstructures are illustrated in the inset. In addition to the loose *BO3* and *BO4* units, superstructural units include the boroxol ring (containing 3 boron), the tetraborate unit (containing 8 boron), and the diborate unit (containing 4 boron).

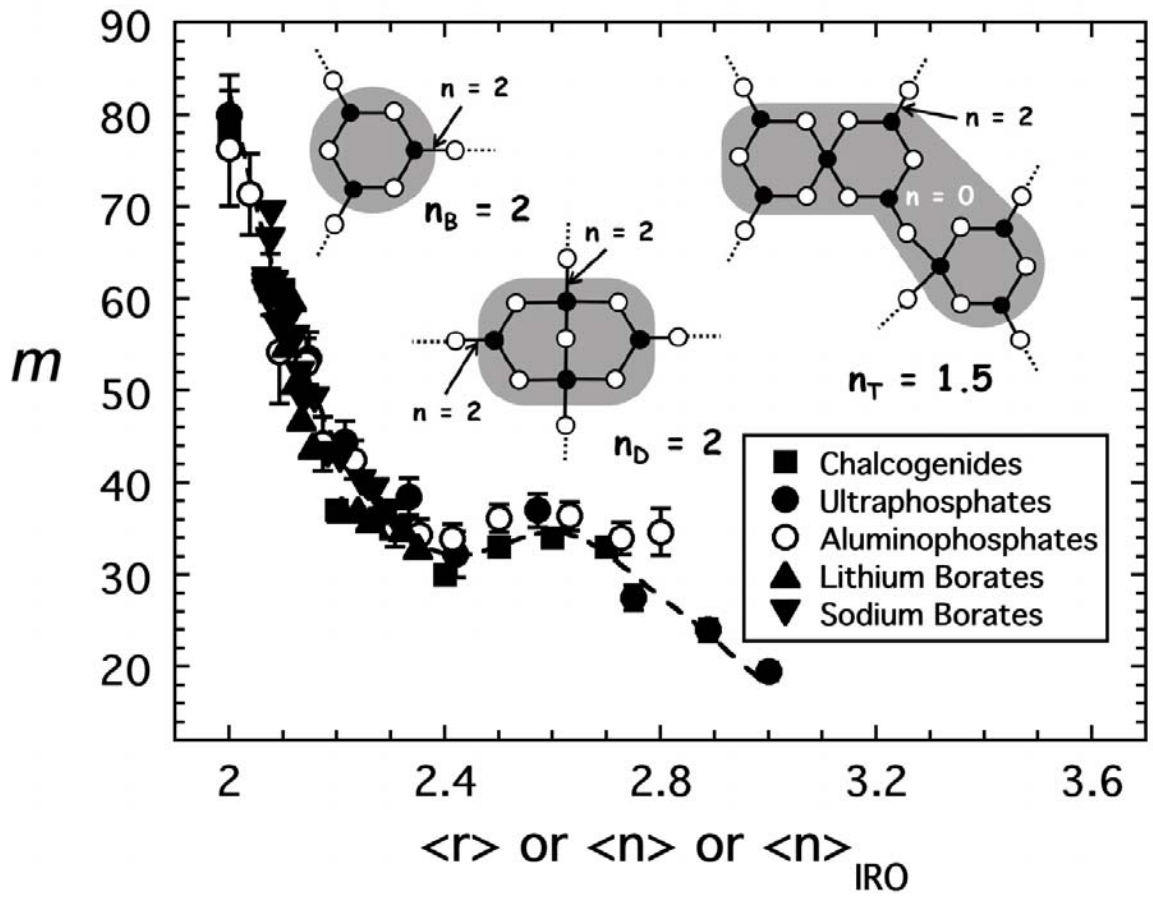

Figure 4

The fragility of Li and Na-borate glasses[30,31] are shown to collapse onto the same curve of Fig. 1 provided the average bond number is defined to include the IRO of the network as discussed in the text. Inset illustrates how the superstructural units in the borate network are coarse-grained into equivalent network nodes.